Applied Catalysis B: Environmental 152–153 (2014) 360–369

Contents lists available at ScienceDirect

Applied Catalysis B: Environmental

journal homepage: www.elsevier.com/locate/apcatb

Partial oxidation of methane over bifunctional catalyst I. In situ formation of Ni^0/La_2O_3 during temperature programmed POM reaction over $LaNiO_3$ perovskite

Tri Huu Nguyen[a,b,c,*], Agata Łamacz[a,**], Patricia Beaunier[d], Sylwia Czajkowska[a], Marian Domański[a], Andrzej Krztoń[a], Tiep Van Le[e], Gérald Djéga-Mariadassou[f]

[a] Centre of Polymer and Carbon Materials Polish Academy of Sciences, Marii Curie Skłodowskiej 34, 41-819 Zabrze, Poland
[b] Silesian University of Technology, Faculty of Chemistry, M. Strzody 9, 44-100 Gliwice, Poland
[c] Saigon University, Faculty of Education of Natural Sciences, 273 An Duong Vuong Dis.5, HCMC, Vietnam
[d] Laboratoire Réactivité de Surface, University Pierre et Marie Curie, Paris 6, UMR 7197-CNRS, 3 rue Galilée, 94200 Ivry, France
[e] IAMS, Vietnam Academy of Science and Technology (VAST), 1 Mac Dinh Chi Dis.1, HCMC, Vietnam
[f] On leave from University Pierre and Marie Curie, Paris, France

ARTICLE INFO

Article history:
Received 17 October 2013
Received in revised form 23 January 2014
Accepted 27 January 2014
Available online 4 February 2014

Keywords:
$LaNiO_3$ perovskite
Ni^0/La_2O_3
NiO demixing
POM
Syngas

ABSTRACT

The transformation of perovskite to an oxide-supported metal during reaction of partial oxidation of methane (POM) has been very often cited in literature as the "reduction" of the perovskite, without any detailed mechanism. In this work, the in situ transformation of initial $LaNiO_3$ perovskite to Ni^0/La_2O_3 was studied under flowing CH_4/Ar and $CH_4 + O_2$/Ar (POM mixture) in temperature-programmed conditions. The catalyst was characterized before, during and after these experiments using X-ray diffraction (XRD), thermogravimetric analysis (TGA) and high resolution transmission electron microscopy (HRTEM/EDS) with Fast Fourier Transform (FFT) and Reverse FFT. Total oxidation of methane over $LaNiO_3$ and lanthanum oxide (La_2O_3), as well as formation of syngas over the resulting Ni^0/La_2O_3 catalysts, were studied for interpreting the three-step evolution of $LaNiO_3$ to Ni^0/La_2O_3, and evidencing NiO demixing from perovskite. A new global kinetic model of POM process over the final bifunctional Ni^0/La_2O_3 catalyst was described.

1. Introduction

Two methane processes, catalytic "total" oxidation of methane to CO_2 and H_2O and its "partial" oxidation (POM) to CO and H_2 utilize dioxygen as oxidant, but they are mechanistically completely different. This diversity arises from both different O_2/CH_4 ratios and catalysts used in these reactions. It will be shown in this paper that the total oxidation of methane is included in the overall mechanism of POM reaction.

Various catalysts have been studied in POM reaction [1–4] but the most popular are nickel catalysts. The goal of this work was to investigate for the first time, the detailed in situ "transformation" of $LaNiO_3$ perovskite (used as precursor) to Ni^0/La_2O_3 looking to (i) the particular steps of Ni^0/La_2O_3 formation and (ii) the optimal Ni^0 dispersion and its contact with the lanthanum oxide. Takehira et al. [1] have found that Ni supported on perovskites, prepared by solid phase crystallization, showed high activity and selectivity and a very low coke formation. The authors have attributed good catalyst performance to high dispersion and stability of Ni particles on perovskite. Hayakawa et al. used $CaTi_{1-x}Ni_xO_3$ as catalyst precursor for POM reaction [5]. The authors have reported that they obtained in situ highly dispersed metallic nickel during the reaction, what resulted in high activity and stability of the catalyst. Pereniguez et al. [2] have studied $LaNiO_3$ as catalyst precursor for Ni^0/La_2O_3. They also formed in situ the metallic nickel during POM reaction.

The transformation of perovskite to Ni^0/La_2O_3 in temperature-programmed reduction (TPR) by H_2 conditions is quite different from the transformation of the perovskite in flowing POM mixture, which is the main objective of the present work. Gallego et al. [6] have shown that after methane dry reforming, the average size of nickel particle was smaller when the catalyst was used without pre-treatment by H_2, than when it was pre-reduced under hydrogen. In previous papers they have shown that $LaNiO_3$ perovskite used as catalyst precursor leads to a very active catalyst for the CO_2

* Corresponding author at: Saigon University, Faculty of Education of Natural Sciences, Vietnam. Tel.: +84903114964.
** Corresponding author at: Centre of Polymer and Carbon Materials Polish Academy of Sciences, 41-819 Zabrze, Poland. Tel.: +48322716077.
E-mail addresses: huutri_sgu@yahoo.com (T.H. Nguyen), agata.lamacz@cmpw-pan.edu.pl (A. Łamacz).

0926-3373/$ – see front matter © 2014 Elsevier B.V. All rights reserved.
http://dx.doi.org/10.1016/j.apcatb.2014.01.053

reforming of CH_4 [7,8]. In the TPR experiment, they have Ni^0 and La_2O_3 by "destruction" of $LaNiO_3$. NiO has not been observed as intermediate. There is no detailed description of the mechanism of this "destruction". The authors have found that a reducing treatment under hydrogen is not necessary before reaction since the perovskite structure is completely "destroyed" under flowing dry reforming reactants CH_4–CO_2. Consequently, due to the high concentration of CO_2 they also get $La_2O_2CO_3$ instead of La_2O_3. Viparelli et al. [3] have found that $BaZr_{(1-x)}Rh_xO_3$ perovskite pre-reduced under H_2 is less active than the catalyst in situ "reduced" during POM reaction.

In our work the transformation of $LaNiO_3$ to Ni^0/La_2O_3 was more particularly studied in the conditions of POM reaction, i.e. under flowing CH_4/O_2/Ar mixture, where the CH_4/O_2 ratio was 2/1. The temperature at which $LaNiO_3$ transform to Ni^0/La_2O_3 was determined during catalytic runs carried out in the temperature-programmed conditions. In order to check the stability and activity of Ni^0/La_2O_3, the POM reaction was also conducted in isotherm. Additionally, for sake of interpretation of experimental data, $LaNiO_3$ and La_2O_3 were also tested in the reaction of methane total oxidation.

2. Experimental

2.1. Synthesis of $LaNiO_3$ perovskite

Bulk perovskite $LaNiO_3$ was synthesized by a modified Pechini method. First, a quantity of citric acid (99.6%, Acros) was dissolved in deionizated water, leading to a 0.15 M clear solution. Then, the adequate amounts of both lanthanum nitrate hexahydrate (POCH, Pure P.A.) and nickel nitrate hexahydrate (99.9985%, ABCR Gmbh & Co.) were added to the solution of citric acid which was stirred for 1 h at room temperature. Afterward, the mixture was heated to 60 °C and stirred for 2 h in order to obtain a stable mix complex. An amount of ethylene glycol (99%, POCH) was then added to the solution, and the stirring was carried out for 1 h at 60 °C. The solution was subsequently stirred and evaporated at 90 °C in order to obtain viscous syrup. Next, the syrup was dried at 90 °C for 10 h in a dryer. The resulting resin or foam was then decomposed at 220 °C for 3 h. The final solid was crushed and calcined in static air at 800 °C for 6 h.

2.2. Catalyst characterization

The catalysts were characterized using the X-Ray diffractometer (TUR-M62) with copper anticathode (λ = 1.54 Å), 34 kV voltage and 25 mA current. The XRD patterns were acquired for 2θ angles ranging from 20 to 85°, with 0.03° steps.

The specific surface area (SSA) of catalysts was determined using the BET method. The measurements were carried out on the Autosorb (Quantachrom Instruments version 2.0). The N_2 adsorption–desorption curves were acquired for the sample cooled to −196 °C. Before N_2 adsorption the samples were degassed at 250 °C for 13 h.

The transformation of $LaNiO_3$ was carried out in flowing 1 vol.% CH_4/Ar.

The relative stabilities of the $LaNiO_3$ perovskite in reducing atmospheres were determined by thermogravimetric reduction in a 1% CH_4/Ar gas mixture. The measurements were made using a Derivatograph Q-1500 thermogravimetric analyzer. The weight change of the samples (ca. 100 mg) was recorded upon heating at a rate of 5 °C/min up to 900 °C in a stream of 100 ml/min gas mixture.

Characterization of the catalytic material before and after runs was done by HRTEM on a JEOL JEM 2010 UHR equipped with a LaB_6 filament and operating at 200 kV with the images collected with a 4008 × 2672 pixels CCD camera (Gatan Orius SC1000) coupled with the DIGITAL MICROGRAPH software. Fast Fourier Transform (FFT) from crystal to diffraction and Reverse FFT (RFFT) from diffraction back to crystal image were performed. The chemical analysis was obtained by a selected energy-dispersive X-ray spectroscopy (EDS) microanalyser (PGT-IMIX PC) mounted on the microscope (the penetration depth of the analysis sphere was 1 micron). The sample was crushed and dispersed in ethanol. A drop of this solution was deposited on a lacey carbon film-copper grid for the HRTEM observations.

2.3. Catalytic tests

Catalytic runs were carried out in a temperature programmed mode (temperature programmed surface reaction (TPSR) or temperature programmed transformation of material (TPT)) in a continuous gas flow, fixed bed U-shape quartz reactor of 18 mm inner diameter, at atmospheric pressure. The amount of $LaNiO_3$ sample used for TPT experiments was 0.3 g. The temperature was raised from room temperature to 900 °C with 5 °C/min heating rate. The total flow rate of reaction mixture was 100 ml/min. The GHSV was 20,000 h^{-1}. The reaction mixture for POM reaction consisted of 1 vol.% CH_4 and 0.6 vol.% O_2 and argon as a balance. The reactants and products were analyzed using a gas chromatograph (GC) equipped with a thermal coupled detector (TCD). The catalytic runs of methane total oxidation (TO) were carried out over $LaNiO_3$ and La_2O_3 in flowing 1 vol.% CH_4/6 vol.% O_2/Ar. Blank runs for CH_4 total oxidation were performed both in an empty reactor and the reactor filled up with quartz wool.

3. Results and discussion

3.1. Characterization of $LaNiO_3$ before reaction

The first objective of this work is the detailed characterization (composition, texture, structure) of the initial $LaNiO_3$. The specific surface area of the initial $LaNiO_3$ was 3 m^2/g after 6 h calcination at 800 °C. The corresponding XRD pattern of $LaNiO_3$ is shown in Fig. 1. The diffraction lines reveal the presence of a rhombohedral single phase in agreement with the JCPDS file 88-0633. The by XRD identification is in agreement with the HRTEM/EDS observations (Figs. 2 and 3), which proved that $LaNiO_3$ is pure and well crystallized.

On the TEM image of $LaNiO_3$ at low magnification (Fig. 2), EDS spectra corresponding to zones 2–4 are reported. The EDS spectrum for zone 1 was the same as for zones 2–4. The EDS spectra

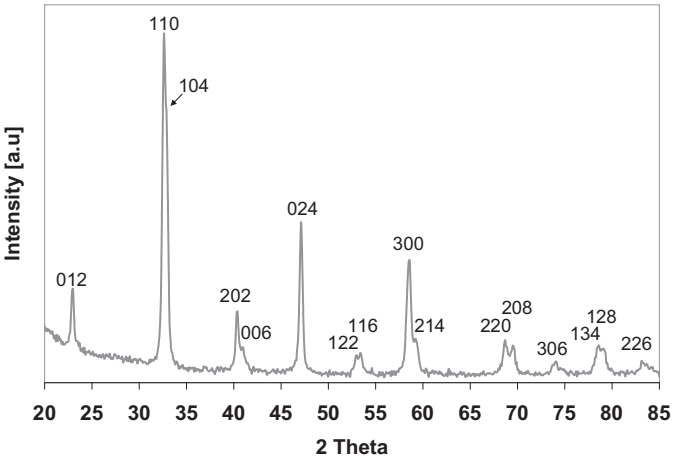

Fig. 1. The XRD pattern of $LaNiO_3$ after calcination at 800 °C.

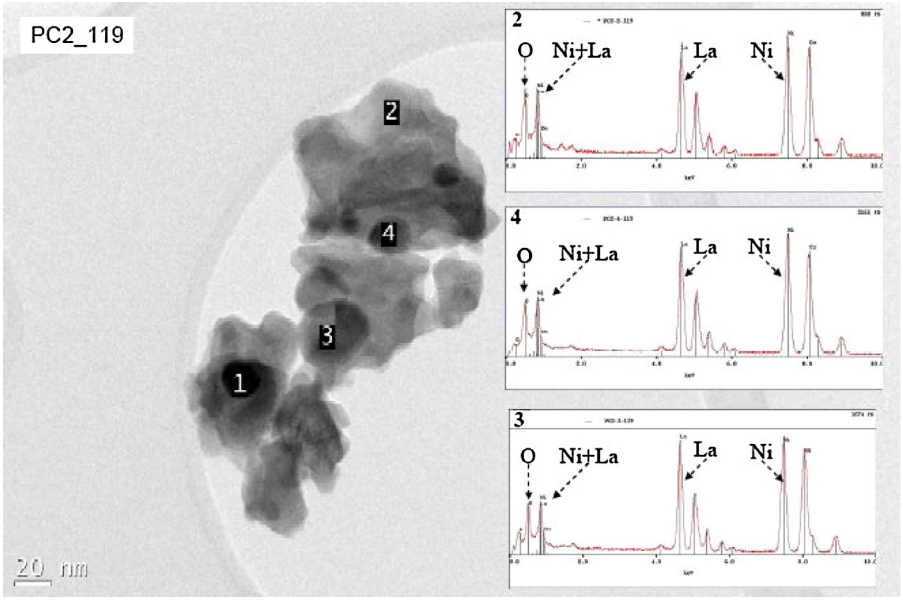

Fig. 2. HRTEM/EDS of $LaNiO_3$.

are showing the same O, Ni and La detected X-lines (keV) and same intensity peaks of these perovskite elements. These data show that the initial $LaNiO_3$ perovskite is quite pure (EDS) with smaller particle sizes from about 20 to 40 nanometers (TEM).

The lattice structure and fast Fourier transform (FFT) using HRTEM on a new zone representative of an aggregate of several perovskite crystals is shown in Fig. 3. The "a" and "b" particles selected on the upper image of Fig. 3, were chosen to obtain, on time during the HRTEM experiment, their fast Fourier transform. This calculated diagram is representative of the electron diffraction pattern (reciprocal lattice), whose diffracted spots indexes have the same values that Miller indexes of the direct lattice planes diffracting in the real crystal (HRTEM image). These diffracting planes are perpendicular to the crystal image (HRTEM image) and to the reciprocal direction of FFT pattern.

- the FFT of the "a" zone, corresponds to the [4 2 $\bar{1}$] zone axis (crystal lattice direction perpendicular to the HRTEM image) and the [0 1 2]* reciprocal direction corresponds to the (0 1 2) lattice planes of the crystal, whose $d_{012} \sim 0.37$ nm, which is in agreement with perovskite JCPDF file;
- the FFT of crystal "b" only shows the [1 0 4]* reciprocal direction corresponding to the lattice spacing $d_{104} = 0.264$ nm of perovskite, as directly measured on the crystal image in agreement with the JCPDF file.

3.2. Transformation of $LaNiO_3$ in flowing CH_4/Ar

The experiment of temperature programmed transformation (TPT) of $LaNiO_3$ under flowing CH_4/Ar was performed in order to observe the behavior of perovskite in the atmosphere of hydrocarbon, which has also been studied in reactions of total and partial oxidation. This kind of experiment was performed in order to show us the ability of perovskite to reduce and transform to Ni^0 and La_2O_3 with subsequent oxidation of CH_4 to CO_2 and H_2O. The TPT experiment was supported by the TGA of perovskite, also carried out in flowing CH_4/Ar.

The profile of temperature programmed transformation (TPT) of $LaNiO_3$ in flowing CH_4/Ar is presented in Fig. 4. Three different temperature ranges of catalyst behavior can be observed. In the first region, up to 630 °C, no reaction is occurring. However, from 550 °C (line no. 1), a small decrease in CH_4 can be observed. The total oxidation (TO) of CH_4 is occurring from 630 °C (line no. 2). Methane is consumed and CO_2 is formed Eq. (1). The total oxidation of CH_4 also yields H_2O, but it was not measured during experiments. The total oxidation of CH_4 utilizes oxygen from the bulk of $LaNiO_3$, which means that $LaNiO_3$ is being reduced by methane. The rate of CO_2 formation is the highest at 670 °C (line no. 3). At this temperature Ni^0 is formed, allowing formation of CO and H_2. From line no. 3, i.e. above 670 °C, we can still observe CO_2, indicating continuous catalyst reduction (and hence CH_4 total oxidation). Whereas the presence of CO and H_2 are assigned to the occurrence of dry and steam reforming reactions, utilizing CO_2 and H_2O respectively Eqs. (2) and (3).

$$CH_4 + 2O_2 = CO_2 + 2H_2O \quad (1)$$

$$CH_4 + CO_2 = 2CO + 2H_2 \quad (2)$$

$$CH_4 + H_2O = CO + 3H_2 \quad (3)$$

The maximal CH_4 consumption is observed at 705 °C (line no. 4). From this moment CH_4 returns to its initial concentration, which is caused by (i) the end of total oxidation of methane due to the absence of oxygen species in the catalyst and (ii) the end of SR and DR of methane due to the lack of CO_2 and H_2O. On the basis of the diffractogram and the JCPDS files 040850 (Ni), 050602 (La_2O_3) and 361481 ($La(OH_3)$), we can conclude that $LaNiO_3$ was completely transformed to Ni^0 and La_2O_3 (Fig. 5).

In order to prove this transformation, the TGA was carried out in the same conditions as the TPT experiment. The thermogravimetric analysis in flowing CH_4/Ar over $LaNiO_3$ is shown in Fig. 6. It can be observed that at the beginning of TGA, the mass of the sample decreases by approximately 2%. It is probably due to the loss of adsorbed H_2O. The subsequent increase of sample mass (up to 280 °C) can be due to adsorption of CH_4 from the gas phase. Next, from 330 to 550 °C, the mass of the $LaNiO_3$ sample slightly decreases, which can be ascribed to desorption of physisorbed CH_4. The subsequent mass loss, which is observed from 550 °C proceeds in three steps. The first decrease of sample mass is observed between 550 and 630 °C (line nos. 1 and 2), and corresponds to the reduction/demixing of $LaNiO_3$ to La_2NiO_4 Eq. (4). On the TPT profile (Fig. 4), in this temperature range, CH_4 consumption was observed. However, no CO_2 was detected. In such a case, it can be

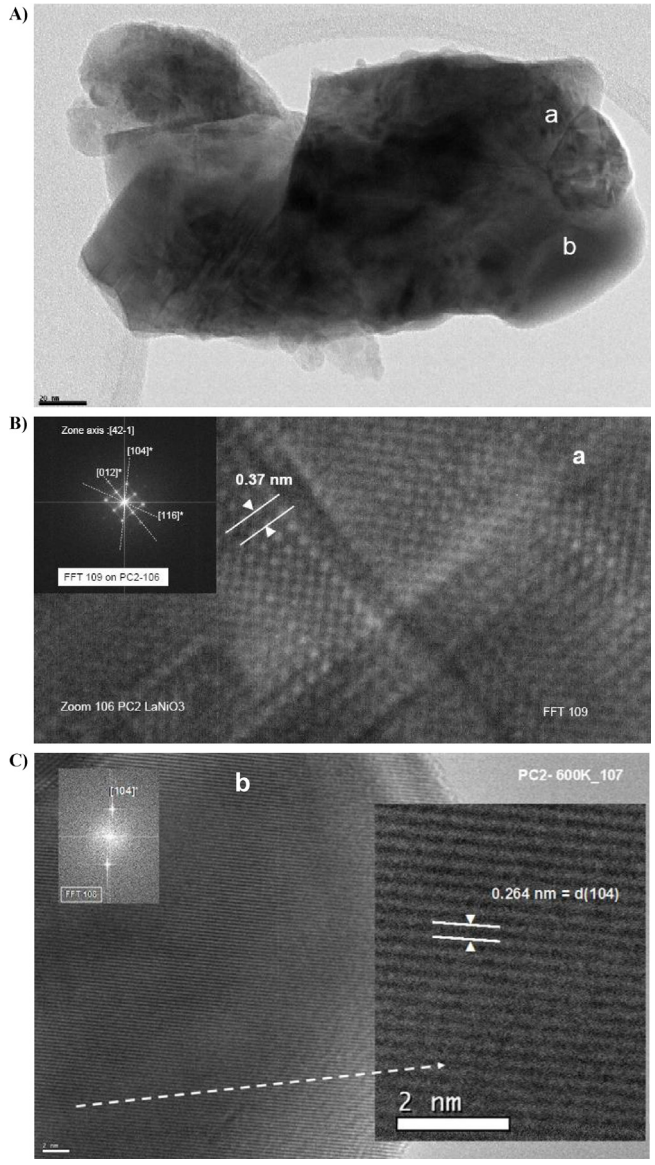

Fig. 3. HRTEM/FFT of the $LaNiO_3$: (A) the lattice structure, (B) and (C) FFT, crystal symmetry and orientation of perovskite "a" and "b" crystals in agglomerate.

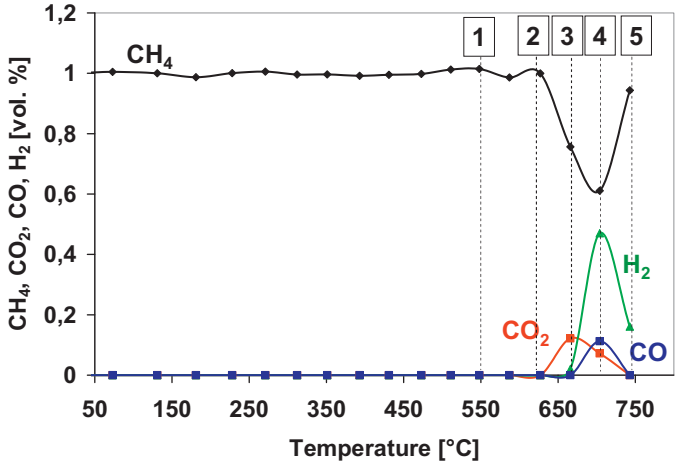

Fig. 4. TPT of $LaNiO_3$ (vol.% of CH_4 (♦), CO_2 (•), CO (▲) and H_2 (■)).

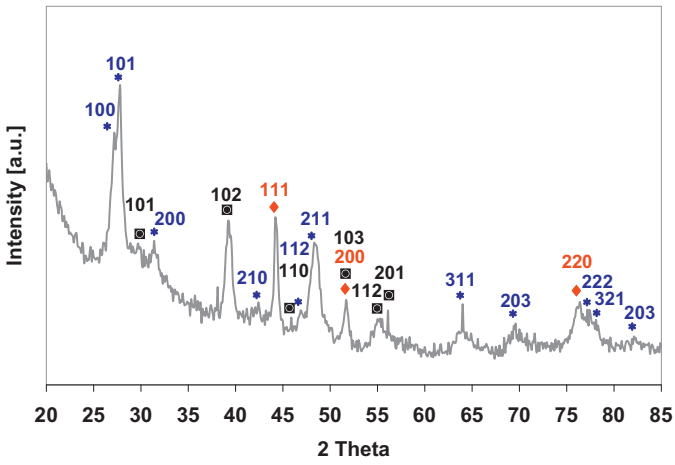

Fig. 5. XRD of the catalyst after TPT experiment (Ni (♦), La_2O_3 (♦), $La(OH)_3$ (*)).

presumed that the rate of $LaNiO_3$ transformation to La_2NiO_4 is very low. Moreover, produced CO_2 may adsorb on catalyst to yield carbonate species. The second reduction step observed on TGA profile, between 630 and 680 °C (line nos. 2 and 3, Fig. 6), corresponds to the demixing of La_2NiO_4 to La_2O_3/NiO and NiO to $NiO_{(1-x)}$ (Eqs. (5) and (6). It can be observed on TPT profile (Fig. 4), that in this temperature region CH_4 consumption is significant and CO_2 is formed. The third reduction step on TGA profile (Fig. 6), between 680 and 770 °C (line nos. 3 and 4), corresponds to complete reduction $NiO_{(1-x)}$ to Ni^0 Eq. (7). Then, from 770 °C (line no. 4), the weight of the sample increases, which is probably due to methane dehydrogenation over Ni^0, followed by carbon deposition. The complete reduction of $LaNiO_3$ to Ni/La_2O_3 was confirmed by the XRD of the sample after TPT experiment carried out in flowing CH_4/Ar (Fig. 5). In the case of $LaNiO_3$ treatment in H_2, only two steps of catalyst reduction were reported [9,10]

$$2LaNiO_3 + 1/4CH_4 \rightarrow La_2NiO_4 + NiO + 1/4CO_2 + 1/2H_2O \quad (4)$$

$$La_2NiO_4 \rightarrow La_2O_3 + NiO \quad (5)$$

$$NiO + x/4CH_4 \rightarrow NiO_{(1-x)} + x/2H_2O + x/4CO_2 \quad (6)$$

$$NiO_{(1-x)} + (1-x)/4CH_4 \rightarrow Ni + (1-x)/4CO_2 + (1-x)/2H_2O \quad (7)$$

3.3. *Total oxidation of CH_4 over $LaNiO_3$ and La_2O_3*

The TPSR profile of the total oxidation of methane over $LaNiO_3$ is shown in Fig. 7. It reveals that the total oxidation of methane starts from 440 °C (line no. 1). It corresponds to the consumption of CH_4

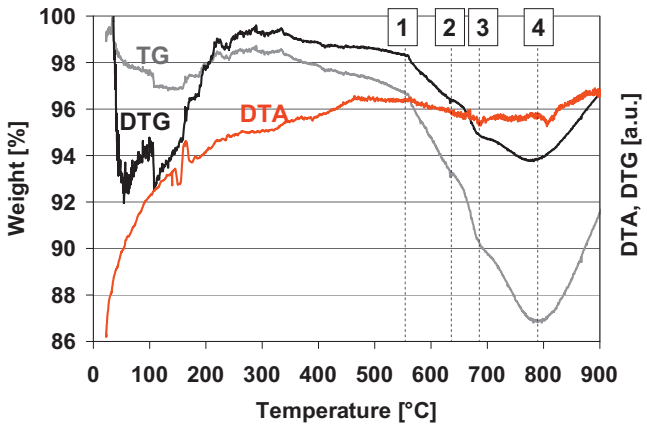

Fig. 6. TGA of $LaNiO_3$ in flowing CH_4/Ar.

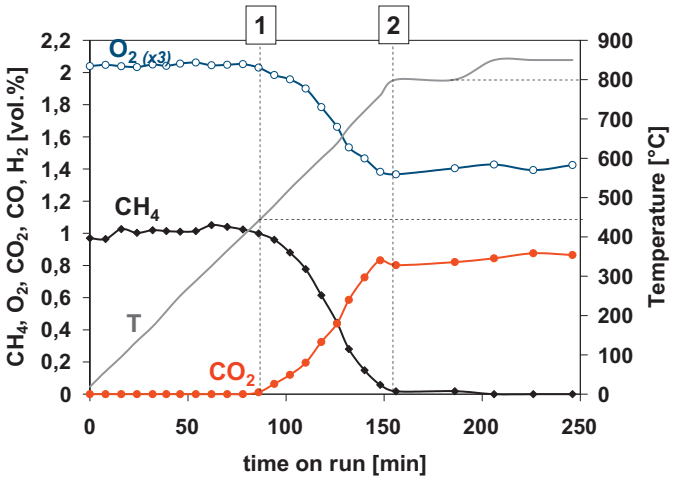

Fig. 7. TPSR of methane total oxidation over $LaNiO_3$ (vol.% of CH_4 (♦), O_2 (○), CO_2 (●), CO and H_2 were not produced).

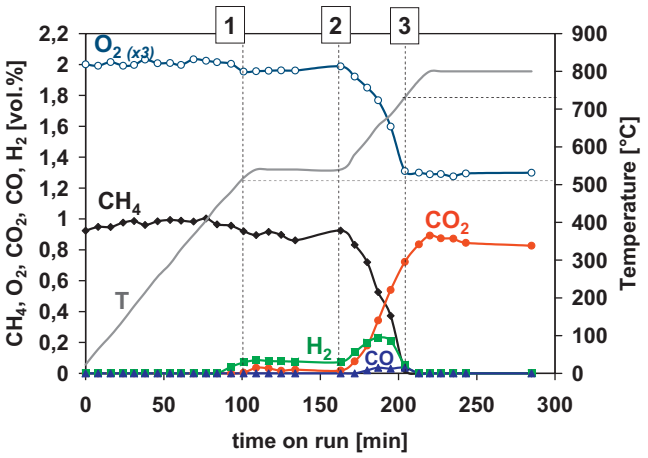

Fig. 9. TPSR of methane total oxidation over La_2O_3 (vol.% of CH_4 (♦), O_2 (○), CO_2 (●), CO (▲) and H_2 (■)).

and O_2 with simultaneous formation of CO_2 and H_2O (water was not measured) Eq. (1). From 800 °C (line no. 2), methane is completely consumed. At 100% conversion of CH_4, the yield of CO_2 was only 90%. About 10% of CO_2 could be adsorbed as carbonate species on perovskite surface [11,12]. The reaction of methane total oxidation was then carried out at 800 °C for 30 min. and at 850 °C for 60 min. One can observe that during these isotherms the catalyst was stable. During the oxidation of methane over the $LaNiO_3$, neither CO nor H_2 were produced. As was confirmed by the XRD of $LaNiO_3$ after total oxidation of methane (Fig. 8), the perovskite was not destroyed. However, a small sintering of the $LaNiO_3$ particles was observed. The grain size of $LaNiO_3$ before and after methane total oxidation, calculated from the (1 1 1) reflex using Scherrer's equation was 60 and 67 nm, respectively.

The TPSR profile of CH_4 total oxidation over La_2O_3 is shown in Fig. 9. It can be observed that total oxidation of CH_4 over this catalyst is very similar to that obtained for $LaNiO_3$ perovskite but the temperature at which the reaction starts (520 °C, line no. 1) is higher, which is due to the absence of nickel. The reaction was carried out at 540 °C for 50 min. The formation of CO_2 during this isotherm indicates the beginning of methane total oxidation, which also yields oxygen vacancies "□" on the catalyst surface. According to Mars and Van Krevelen mechanism [13], the presence of these vacancies enables water dissociation Eq. (8) and formation of H_2, which was is detected in the gas phase during methane total oxidation over La_2O_3. Hence, the formation of H_2 can be assigned to catalytic dissociation of water, at the molecular level, over La_2O_3. In contrary to

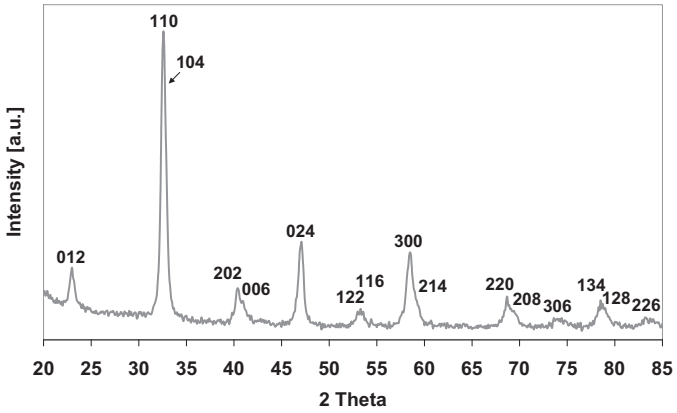

Fig. 8. XRD of $LaNiO_3$ after total oxidation of CH_4.

$LaNiO_3$, small amounts of H_2 are produced over La_2O_3 at temperatures ranging from 500 to 700 °C. As the temperature is increased from 540 °C, the rate of CO_2 formation due to CH_4 total oxidation and H_2 production due to H_2O dissociation increases. The La_2O_3 catalyst could be also able to catalyze the water gas shift reaction (WGS); however, this kind of study will be performed in the future. According to [14], H_2O can dissociate over the CeO_2 or $CeZrO_2$ Eq. (8).

$$H_2O + □ \rightarrow □O + H_2 \quad (8)$$

According to Haber and Turek [15], the total oxidation is appearing at the surface as the result of the dynamic equilibrium between the metal oxide and the gas phase oxygen. The selective oxidation of hydrocarbon by the lattice oxygen to oxygen containing compounds (acids, aldehydes or alcohols) was also considered but it is not occur in our case. In presented case, methane oxidation yields only CO_2 and H_2O. The complete conversion of methane over La_2O_3 occurs at lower temperature (730 °C, line no. 3) when compared to $LaNiO_3$.

The results of catalytic runs of methane total oxidation over $LaNiO_3$ and La_2O_3 (Figs. 7 and 9) have shown that the reaction starts at about 450–520 °C, and the hydrocarbon is completely consumed at about 800 °C. These results are similar to those presented by Hu et al. [16]. Neither CO nor H_2 was detected by the authors, due to the absence of metallic active sites, which are responsible for reactions leading to syngas.

As was proved by XRD analysis, the $LaNiO_3$ (Fig. 8) and La_2O_3 (not shown) did not decompose during catalytic runs of CH_4 total oxidation. This characteristic feature of La_2O_3 is fundamental for establishing the catalytic model of POM reaction over Ni^0/La_2O_3.

Blank runs of methane total oxidation performed in temperature-programmed conditions in an empty reactor proved that the reaction is not occurring. Similar blank runs with the reactor filled up with quartz wool showed negligible CH_4 conversion above 800 °C.

3.4. Catalytic POM reaction

The TPSR profile of the POM reaction over $LaNiO_3$ is presented in Fig. 10. The catalyst is inactive below 350 °C. Above this temperature, up to 600 °C (between line nos. 1 and 2), the total oxidation of CH_4 is occurring. Both the methane and O_2 are consumed and CO_2 is formed. The total oxidation of CH_4 results also in H_2O formation, not measured during experiments. This is consistent with what has just been shown above: $LaNiO_3$, the catalyst is able to proceed to methane total oxidation. The consumption of oxygen from the gas

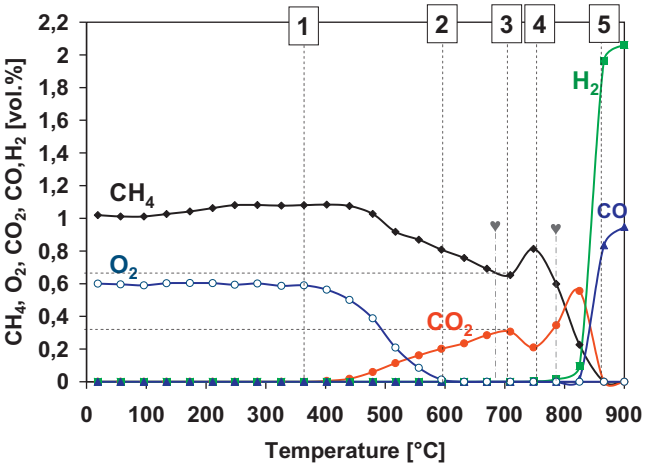

Fig. 10. TPSR profile of POM reaction over $LaNiO_3$ (vol.% of CH_4 (♦), O_2 (○), CO_2 (•), CO (▲) and H_2 (■)). The XRD analyses of the catalyst were made at 680 and 780 °C (♥).

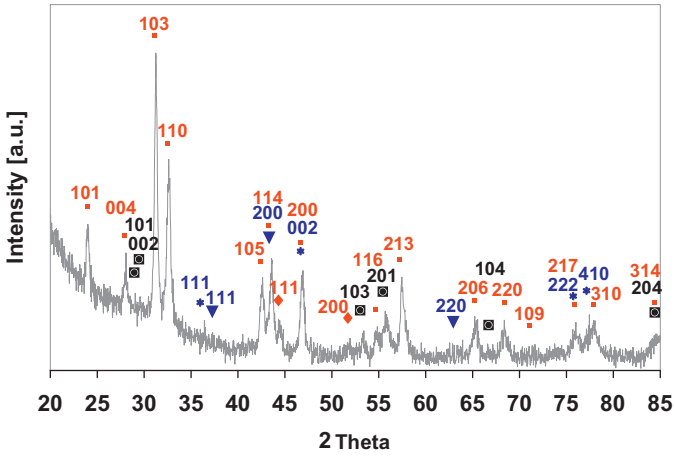

Fig. 12. XRD patterns of the ex-$LaNiO_3$ collected during POM TPSR at 780 °C, proving formation of NiO and La_2O_3 (Ni (♦), NiO (▼), La_2NiO_4 (■), La_2O_3 (■), $La(OH)_3$ (*)).

phase is complete from 600 °C. It is expected that in this temperature range CO_2 and CH_4 concentrations are constant. However, in presented case the CO_2 is rising and CH_4 continues to be consumed. It means that methane undergoes its total oxidation to CO_2/H_2O. What is the reason for that?

- Firstly, we have to take into account the results of XRD analysis of the material at 680 °C (Fig. 11), showing the presence of "NiO + La_2NiO_4 + $LaNiO_{3(residual)}$" and evidencing demixing of nickel oxide from perovskite with subsequent formation of the dilanthanum nickel oxide Eq. (9);

$$2LaNiO_3 \rightarrow La_2NiO_4 + NiO + \tfrac{1}{2}O_2 \quad (9)$$

- Secondly, the demixing is not completed at 600–700 °C (between line nos. 2 and 3; Fig. 10) and $LaNiO_3$ is still remaining (proved by XRD; Fig. 11all lines are in agreement with JCPDS files (88-0633 ($LaNiO_3$), 00-004-0835 (NiO) and 01-070-0509 (La_2NiO_4));
- Finally, methane consumption and CO_2 formation up to 700 °C are corresponding to the stoichiometry of the reaction of CH_4 total oxidation Eq. (1), but the amount of oxygen consumed completely from the feed is not sufficient. Therefore, some amount of oxygen for CH_4 total oxidation has been provided by the $LaNiO_3$, according to Eqs. (4) and (9).

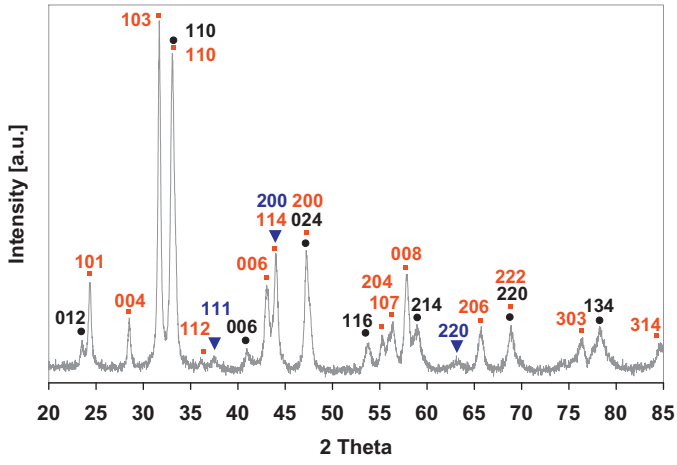

Fig. 11. XRD pattern of the ex-$LaNiO_3$ collected at 680 °C during POM TPSR proving formation of NiO and La_2NiO_4 intermediates (NiO (▼), La_2NiO_4 (■), $LaNiO_3$ (•)).

Moreover, since neither CO nor H_2 is formed, we may assume NiO reduction to NiO_{1-x} (as has been previously defined, syngas formation needs the presence of Ni^0). This is the case occurring in the temperature region between line nos. 2 and 3: CO_2 is increasing without formation of CO/H_2, owing to partial reduction of NiO to NiO_{1-x} and occurring together with methane oxidation, like in the "fuel reactor" of chemical looping combustion" (CLC) process [17]. Hence, as far as the catalyst is in its oxidized state in the reaction mixture of POM, the total oxidation of CH_4 is occurring.

In the next temperature range, between line nos. 3 and 4, i.e. up to 750 °C, there is less perovskite and consequently less NiO is demixed from $LaNiO_3$ Eq. (9). The CO_2 is decreasing and methane is increasing again due to the end of initial perovskite and to the beginning of NiO demixing from La_2NiO_4, which yields La_2O_3 Eq. (5) and NiO_{1-x} Eq. (6) as far there is no CO nor H_2 production. The demixing of NiO from La_2NiO_4 was proved by XRD analysis of sample collected during POM–TPSR at 780 °C (Fig. 12). As is shown on the diffractogram, there are still reflexes of La_2NiO_4 but one can also observe the presence of La_2O_3 and NiO phases. Moreover, the reflexes of $La(OH)_3$ are visible, which can be a result of catalyst exposure to the moisture after reaction [18,19]. However, it cannot be excluded, that the presence of $La(OH)_3$ was a result of catalyst reaction with H_2O [18] (formed during catalyst reduction by CH_4).

$$La_2NiO_4 \rightarrow La_2O_3 + NiO \quad (5)$$

Subsequent increase of temperature (above 750 °C; line no. 4) results in the increase in CO_2, which is due to the beginning of NiO or NiO_{1-x} reduction to Ni^0 according to the theory of hydrocarbon oxidation over oxide [15,20] Eq. (10).

$$4NiO + CH_4 = 4Ni^0 + 2H_2O + CO_2 \quad (10)$$

The presence of zero valent metal enables formation of CO and H_2, which are both detected from 750 °C. The Ni^0 is the active phase for dehydrogenation of methane [21]. The NiO is progressively reduced via NiO_{1-x} to Ni^0 and simultaneously La_2O_3 is formed. The formation of CO and H_2 shows that Ni^0 begins to be active in methane dry and steam reforming. The total oxidation of CH_4 to CO_2 and H_2O continues to turn over on La_2O_3 as shown in Fig. 9. The CO_2 and H_2O are utilized in dry and steam reforming respectively Eqs. (2) and (3). Both reactions occur up to 860 °C (line no. 5) on Ni^0 active sites. Above this temperature the only products detected in the gas phase are CO and H_2, which proves the occurrence of POM reaction Eq. (11). The catalyst over which the DR, SR and POM reactions are occurring is Ni^0/La_2O_3.

$$2CH_4 + O_2 = 2CO + 4H_2 \quad (11)$$

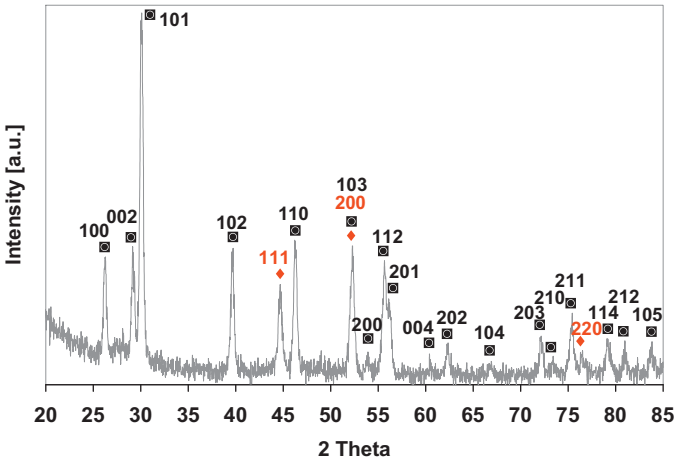

Fig. 13. XRD pattern of the final Ni^0/La_2O_3 catalyst after POM TPSR up to 900 °C (Ni (♦), La_2O_3 (◙)).

The overall transformation of $LaNiO_3$ to Ni^0/La_2O_3 can be summarized by the following 3 reactions i.e. Eqs. (5), (9) and (10) (σ is stoichiometric number of the step) and overall Eq. (12):

$$2LaNiO_3 \rightarrow La_2NiO_4 + NiO + \tfrac{1}{2}O_2 \quad \sigma = 2 \quad (9)$$

$$La_2NiO_4 \rightarrow La_2O_3 + NiO \quad \sigma = 2 \quad (5)$$

$$4NiO + CH_4 = 4Ni^0 + 2H_2O + CO_2 \quad \sigma = 1 \quad (10)$$

$$4LaNiO_3 + CH_4 = 2La_2O_3 + O_2 + 2H_2O + CO_2 + 4Ni^0 \quad (12)$$

The XRD pattern of the ex-$LaNiO_3$ sample collected at 680 °C during POM TPSR (Fig. 11) shows the transformation of $LaNiO_3$ to intermediates, i.e. La_2NiO_4 + NiO. It was shown on the TPSR profile of POM reaction (Fig. 10) that NiO demixing from perovskite is the 1st intermediate step of perovskite transformation to Ni^0/La_2O_3. It has been also proven by the TPT experiment (Fig. 4) and TGA (Fig. 6), both carried out in CH_4/Ar. The NiO demixing from $LaNiO_3$ is followed by another NiO demixing from La_2NiO_4 at higher temperature, which was proved by XRD analysis of the sample collected during POM reaction at 780 °C.

3.4.1. *Characterization of Ni^0/La_2O_3—the "real" catalyst for POM reaction*

The composition of the catalyst after POM was proved by its physico-chemical characterization. During POM reaction, $LaNiO_3$ perovskite was finally transformed to Ni^0/La_2O_3. The SSA of Ni^0/La_2O_3 was 9 m^2/g, and it has been found that it increased by three times in comparison to the initial $LaNiO_3$. Fig. 13 shows the XRD pattern of the catalyst after POM reaction carried out at 900 °C. It clearly shows the presence of Ni + La_2O_3 (JCPDS files 040850 and 050602, respectively). Hence, this catalyst is the one for POM reaction; and therefore, for syngas formation. The typical reflexes of $LaNiO_3$ perovskite and intermediate compounds, i.e. NiO and La_2NiO_4, are not observed on the XRD pattern. Hence, their transformation to Ni^0/La_2O_3 has been proved. Choudhary et al. [19] have shown the XRD of catalyst spent in POM reaction, on which only the reflexes of Ni, La_2O_3 and $La(OH)_3$ are occurring. However, Vella et al. [18] has observed not only such main phases as Ni and La_2O_3, but also side phases, such as NiO, $La(OH)_3$, La_2NiO_4 and $La_2O_2CO_3$. Both Choudhary et al. [19] and Vella et al. [18], have suggested, that $La(OH)_3$ was a result of catalyst exposure to the moisture after POM reaction. However, it cannot be excluded [18], that the presence of $La(OH)_3$ was a result of catalyst reaction with H_2O (formed during catalyst reduction with CH_4) during POM reaction.

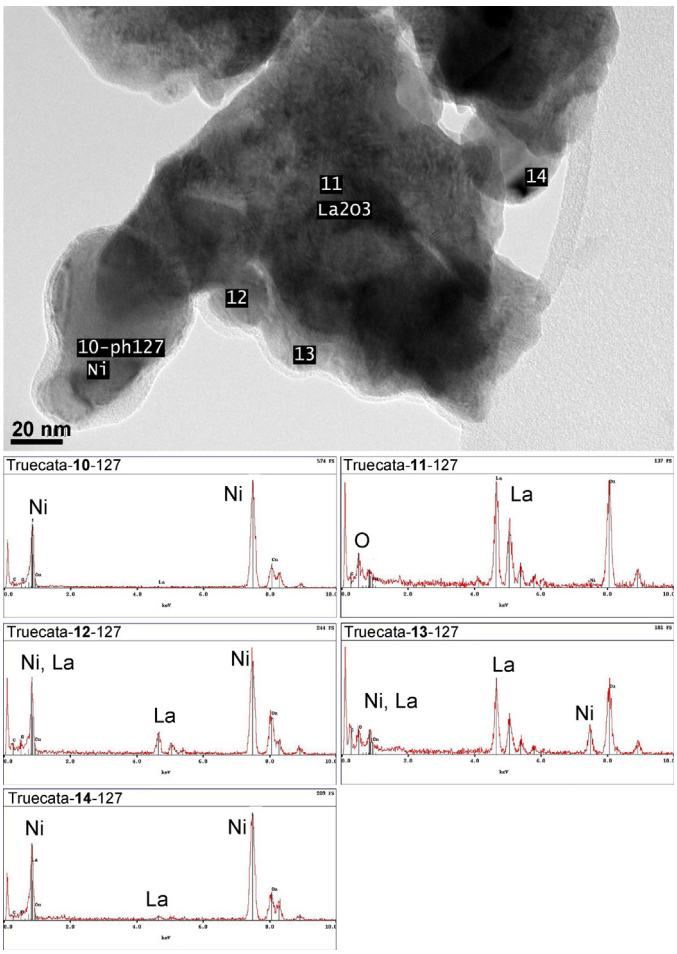

Fig. 14. HRTEM/EDS of Ni^0/La_2O_3 catalyst after POM reaction at 900 °C.

The HRTEM image of the catalyst after POM reaction carried out at 900 °C and EDS spectra corresponding to zones 10–14 are reported in Fig. 14. The EDS spectrum corresponding to zone 11, indicates only the presence of La and O, which is due to La_2O_3. In this zone Ni is not detected; hence, only the pure lanthanum oxide occurs. In contrary, the EDS spectrum of zone 10, on the edge of the agglomerate, shows only the presence of Ni. For this zone, the nickel lattice fringes, and d-spacing of the lattice planes were calculated by FFT and Reverse FFT (RFFT) method (Fig. 15). The RFFT permits coming back from the FFT pattern to the crystal image identifying the domain producing the FFT pattern, as well as its size. It corresponds to the crystal image selected in the square frame where d_{111} was measured. Both the FFT pattern and the image of crystal fringes permit to calculate the d_{111} value, which was 0.203 nm. This value of d_{111} was in agreement with the XRD analysis (Fig. 13).

In the case of EDS spectrum collected for zone 14 (Fig. 14), we can observe high intensity line of Ni and a very low intensity line corresponding to La, which is due to the neighbourhood of La_2O_3 producing some X photons. Nevertheless, in this particles characterized in this zone are pure Ni^0. The EDS spectra for zones 12 and 13 show the overlapping lines of both the Ni (from Ni^0), and La (from La_2O_3), indicating good metal-support proximity. The intensities of the particular X-lines are different from those observed for pure perovskite (Fig. 2). All EDS spectra presented in Fig. 14 show that the initial $LaNiO_3$ has been completely transformed to Ni^0/La_2O_3 during the TPSR experiment carried out in POM mixture up to 900 °C. Let's note that the size of nickel particles, calculated

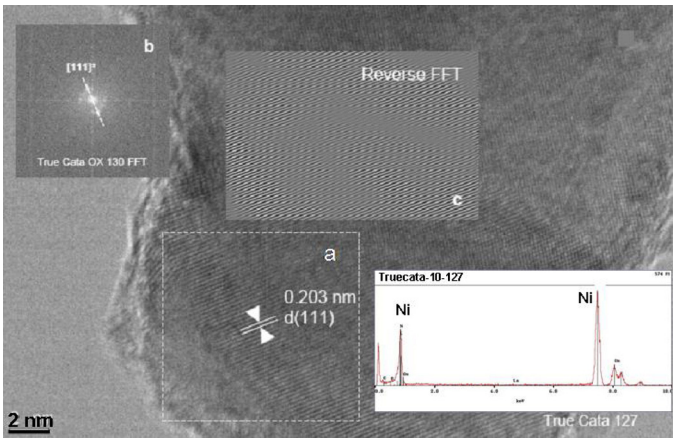

Fig. 15. The HRTEM image of zone 10: the distance between lattice fringes in d_{111} of Ni^0 is 0.203 nm (a); the FFT (b), RFFT (c) and EDS spectrum (d) of area "a".

from the HRTEM image presented in Fig. 14 is less than 20–40 nm. Moreover, Ni particles are in good proximity with the oxide, which is crucial for POM reaction.

By the presented characterization of the initial $LaNiO_3$ and final Ni^0/La_2O_3 it can be emphasized that:

- The initial perovskite is a pure precursor material, which was proved by XRD, HRTEM, FFT and EDS;
- Different solid phases have been characterized during the evolution of this initial $LaNiO_3$ perovskite to the final Ni^0/La_2O_3 material Eq. (13), which is able to catalyze POM reaction:

$$LaNiO_3 \rightarrow NiO + La_2NiO_4 + LaNiO_3 \text{ near } 600\,^{\circ}C \rightarrow \text{pure } Ni^0/La_2O_3 \quad (13)$$

- The presence of pure quasi spherical Ni particles supported over pure La_2O_3 was proved by both the XRD and HRTEM, complemented by FFT and RFFT.
- The good proximity between Ni particles with La_2O_3 has been proved;
- In contrast to literature reports [9,10], from our studies it can be concluded that the so-called "perovskite reduction" occurs in 3 main steps:

a) The demixing of NiO from perovskite, which is leading to formation of dilanthanum nickel oxide intermediate (La_2NiO_4)—proved by XRD;
b) The demixing of NiO from La_2NiO_4, which is leading to formation of La_2O_3—proved by TGA and XRD;
c) The reduction of NiO to Ni^0—proved by TGA and XRD.

The occurrence of these 3 steps was explained, owing to the results of TPSR experiment carried out in POM mixture. In order to understand the process of perovskite transformation to Ni^0/La_2O_3, the reaction of methane total oxidation (TO) to CO_2/H_2O, either over $LaNiO_3$ or La_2O_3 has to be considered. Choudhary et al. [22] have reported that metal (Mn, Co, Fe, Cr, Cu, Ni) doped ZrO_2 catalyst are active in methane total oxidation. Therefore, one cannot discard the possibility of the occurrence of methane total oxidation over Ni doped La_2O_3. Nevertheless, according to [15,20,23,24] when methane combustion is occurring on Ni based catalysts, nickel is either NiO or La_2NiO_4. As a consequence, the methane combustion over Ni^0/La_2O_3 has not been studied. Furthermore it has been shown in this work that La_2O_3 is active for methane combustion at high temperatures and syngas formation is only occurring over Ni^0.

Results presented in our paper are in line with those presented by Choudhary et al. [19] and Preniguez et al. [2] who studied POM reaction over in situ reduced $LaNiO_3$. The catalyst was active for 10 h. In contrary, Vella et al. [18] reported that Ni catalyst derived from $LaNiO_3$ showed very low performance, due to formation of not active species, such as $La(OH)_3$, La_2NiO_4 or $La_2O_2CO_3$. Moreover, they have observed coking on Ni metal and catalyst deactivation.

3.5. The model of catalytic POM reaction over Ni^0/La_2O_3

According to Nishimoto et al. [4] "the synthesis-gas production via the partial oxidation of methane proceeded basically by means of a two step path consisting of complete oxidation to give CO_2 and H_2O, followed by the methane reforming with both CO_2 and H_2O". Nevertheless, as for many other publications in literature, they neither define the nature of active sites, nor the detailed kinetic mechanism. Starting from their conclusion and applying the concepts of classical kinetics, it is first possible, using the definition of the stoichiometric number σ [21,25] to propose the overall POM reaction, starting from 3 main reactions that have occurred during POM TPSR over the bifunctional catalyst (Fig. 10):

$$\text{Total oxidation}: \ CH_4 + 2O_2 = CO_2 + 2H_2O \quad \sigma = 1 \quad (1)$$

$$\text{Dry reforming } (CO_2 \text{ is needed}): \ CH_4 + CO_2 = 2CO + 2H_2 \quad \sigma = 1 \quad (2)$$

$$\text{Steam reforming } (H_2O \text{ is needed}): \ H_4 + H_2O = CO + 3H_2 \quad \sigma = 2 \quad (3)$$

$$\text{Overall equation}: \ 4CH_4 + 2O_2 = 4CO + 8H_2$$

$$\text{or}: \ 2CH_4 + O_2 = 2CO + 4H_2 \quad (11)$$

The values of σ are selected so as to get CO and H_2, as was observed in Fig. 10. This also means that methane and oxygen are completely consumed, as well as CO_2 and H_2O intermediates. In order to obtain 100% selectivity to syngas, POM reactor needs to work with stoichiometric feed of $CH_4/O_2 = 2$. If this ratio is higher, there can be a carbon deposition, because active carbon C* formed on Ni^0 during CH_4 dehydrogenation Eq. (14) would not be scavenged Eq. (16) due to the lack of oxygen (O*), which was delivered by CO_2 and H_2O dissociation also over Ni^0 Eqs. (17) and (18).

$$CH_4 + 5* = C* + 4H* \quad (14)$$

$$H* + H* \rightarrow 2* + H_2 \quad (15)$$

$$C* + O* \rightarrow 2* + CO \quad (16)$$

$$CO_2 + * \rightarrow O* + CO \quad (17)$$

$$H_2O + * \rightarrow O* + H_2 \quad (18)$$

On the basis of the sequence of overall reactions Eqs. (1)–(3), (11) and of the results of TPSR experiment (Fig. 10) and catalyst characterization presented in this work, we proposed a model of classical kinetics (in contrast to micro kinetics [26]) for the POM reaction over Ni^0/La_2O_3 catalyst (Fig. 15). This model assumes the presence of three catalytic cycles, i.e. the total oxidation of methane turning over simultaneously with two coupled catalytic cycles of steam and dry reforming. The reaction of CH_4 total oxidation can occur over La_2O_3 as shown in Fig. 9, producing CO_2 and H_2O, which in turn are consumed by reforming reactions. Both CO_2 and H_2O supply oxygen to the catalyst Eqs. (17) and (18) [27]. The decomposition of CH_4 over metallic nickel active sites (Ni^0, also denoted as "*") is quite recognized now [20] and all elementary steps of dry and steam reforming are occurring over Ni^0. Taking into account in classical kinetics that "one catalytic overall reaction is one catalytic

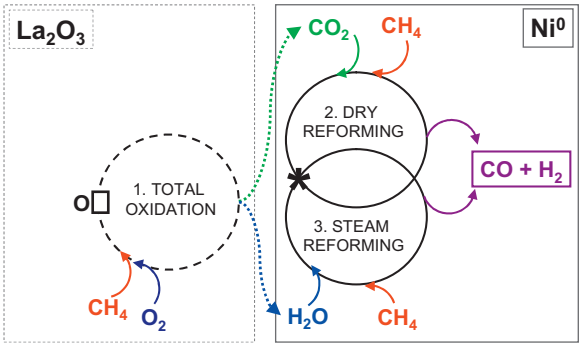

Fig. 16. Classical kinetics model of POM reaction over Ni^0/La_2O_3 bifunctional catalyst: total oxidation of HC occurs on the La_2O_3 over the oxide active site (O□). The active site for DR and SR is zero valent metal (* = Ni^0).

cycle" the following model, will be used as the basis for describing in our next paper, all the elementary steps occurring in each catalytic cycles.

It is worth noting that total oxidation of methane begins by CH_4 activation (reactive dissociative chemisorption) to $CH_3O\square$ + □ OH species [20,28] over surface oxygen species of La_2O_3 (denoted as □ O). These □ O species are linked to the oxide cation. They are subsequently consumed during the reaction of total oxidation, which leads to an "oxygen vacancy" (□). This vacancy is often considered as the reaction "active site". In order to recover the surface oxygen species of La_2O_3, i.e. □ O, the oxygen from the reaction feed dissociates over the oxygen vacancy (□) according to Mars and Van Krevelen mechanism. Dry and steam reforming are occurring over Ni^0 (denoted as *). The active oxygen species, i.e. O*, are coming from CO_2 dissociation in the dry reforming cycle Eq. (17), and from H_2O dissociation Eq. (18) in the steam reforming cycle. The active carbon species (C*) consume O* without distinguishing their origin; hence, the O* are common in both cycles. In classical kinetic it is called a kinetic coupling [25].

The general description of POM reaction can be defined as:

- Methane combustion assisted catalytic reforming over the bifunctional catalyst, which has 2 kinds of sites: (i) the surface oxygen species (□O) of La_2O_3 over which the hydrocarbon undergoes its total oxidation to CO_2 and H_2O, and (ii) the surface Ni^0 active site "*", which is active site for dissociative adsorption of both CO_2 and H_2O leading to formation of O* and CO (in case of DR) or H_2 (in case of SR);
- Kinetic coupling of dry and steam reforming cycles on O* species (where * is Ni^0), after obtaining the real Ni^0/La_2O_3 catalyst from the initial $LaNiO_3$ perovskite in the presence of methane (TPT in CH_4/Ar and POM TPSR experiments).

The model of POM reaction over Ni^0/La_2O_3 catalyst, which is presented in Fig. 16 describes the mechanism of this reaction considering two functions of studied catalyst.

4. Conclusions

The mains objective of this work was to present (i) the detailed in situ transformation of $LaNiO_3$ to Ni^0/La_2O_3 under flowing POM mixture up to 900 °C and (ii) determine new global kinetic model of partial oxidation of methane over the bifunctional Ni^0/La_2O_3 catalyst. The $LaNiO_3$ perovskite was synthesized and characterized using XRD, TGA and HRTEM, with FFT and EDS.

It has been proven that the in situ transformation of $LaNiO_3$ to Ni^0/La_2O_3 occurs in 3 main steps:

1) NiO demixing from perovskite (at 680 °C), leading to the formation of La_2NiO_4;
2) NiO demixing from La_2NiO_4 (at 750 °C);
3) Reduction of NiO to Ni^0 by CH_4, which was consuming oxygen from NiO (reaction occurring in the "fuel reactor" of "chemical looping combustion" of methane using NiO as oxygen carrier, at high temperature ~850 °C) with simultaneous total oxidation of CH_4 to CO_2 and H_2O over La_2O_3.

The resulting Ni^0/La_2O_3 obtained at 900 °C was the real catalyst for dry and steam reforming reactions producing syngas. This bifunctional catalyst was characterized by XRD, HRTEM, EDS, FFT, RFFT, evidencing the surface dispersion and high contact of nickel particles with La_2O_3.

From the results of catalytic runs in temperature-programmed conditions and catalyst characterization after catalytic runs it can be concluded that the mechanism of POM reaction over Ni^0/La_2O_3 consists of three assisted catalytic cycles:

1) Combustion of methane, which is occurring on the "□ O" active sites of La_2O_3;
2) Dry reforming of methane occurring on Ni^0;
3) Steam reforming of methane taking place on Ni^0.

POM reaction is the sum of these three reactions. Neither drastic deactivation of Ni^0/La_2O_3, nor the secondary water gas shift reactions have been observed during catalytic runs of POM reaction.

The presented model of POM reaction will be developed in our next papers, concerning the detailed kinetic description of the sequences of presented here 3 catalytic cycles and the study of the reaction rates, rate constants and activation energy of methane combustion over La_2O_3 as well as methane dry reforming over Ni^0/La_2O_3.

Acknowledgements

Dr. M. Lewandowski is greatly acknowledged for providing lanthanum oxide material.

The government of Vietnam is gratefully acknowledged for the grant (4315/QD-BGDDT) given to Tri Huu Nguyen to realize this work in Poland.

The Faculty of Chemistry Silesian University of Technology and the Centre of Polymer and Carbon Materials, Polish Academy of Sciences are gratefully acknowledged for their experimental support.

References

[1] K. Takehira, T. Shishido, M. Kondo, J. Catal. 207 (2002) 307.
[2] R. Pereniguez, V.M. Gonzalez-DelaCruz, J.P. Holgado, A. Caballero, Appl. Catal. B 93 (2010) 346.
[3] P. Viparelli, P. Villa, F. Basile, F. Trifiro, A. Vaccari, P. Nanni, M. Viviani, Appl. Catal. A 280 (2005) 225.
[4] H.-A. Nishimoto, K. Nakagawa, N.-O. Ikenaga, T. Suzuki, Catal. Lett. 82 (2002) 161.
[5] T. Hayakawa, S. Suzuki, J. Nakamura, T. Uchijima, S. Hamakawa, K. Suzuki, T. Shishido, K. Takehira, Appl. Catal. A 183 (1999) 273.
[6] G.S. Gallego, F. Mondragón, J. Barrault, J.M. Tatibouet, C.B. Dupeyrat, Appl. Catal. A 311 (2006) 164.
[7] C. Batiot-Dupeyrt, G. Valderrama, A. Meneses, F. Martinez, J. Barrault, J.M. Tatibouët, Appl. Catal. A 248 (2003) 143.
[8] C. Batiot-Dupeyrt, G.A. Sierra, F. Mondragon, J. Barrault, J.M. Tatibouët, Catal. Today 107–108 (2005) 474.
[9] M. Stojanovic, R.G. Haverkamp, C.A. Mims, H. Moudallal, J. Jacobson, J. Catal. 165 (1997) 315.
[10] R.M. Garcia de la Cruz, H. Falcon, M.A. Pena, J.L.G. Fierro, Appl. Catal. B 33 (2001) 45.
[11] G. Valderrama, A. Kiennemann, M.R. Goldwasser, Catal. Today 133–135 (2008) 142.
[12] G. Valderrama, M.R. Goldwasser, C. Urbina de Navarro, J. Barrault, J.M. Tatibouët, C. Batiot-Dupeyrt, F. Martinez, Catal. Today 107–108 (2005) 785.
[13] P. Mars, D.W. van Krevelen, Chem. Eng. Sci. 3 (1954) 41 (Special Suppl.).

[14] A. Lamacz, A. Krzton, Int. J. Hydrogen Energy 38 (2013) 8772.
[15] J. Haber, W. Turek, J. Catal. 190 (2000) 320.
[16] R. Hu, R. Ding, J. Chen, J. Hu, Y. Zhang, Catal. Commun. 21 (2012) 38.
[17] T. Mattisson, M. Johansson, A. Lyngfelt, Fuel 85 (2006) 736.
[18] L.D. Vella, J.A. Villoria, S. Specchia, N. Mota, J.L.G. Fierro, V. Specchia, Catal. Today 171 (2011) 84.
[19] V.R. Choudhary, B.S. Uphade, A.A. Belhekar, J. Catal. 163 (1996) 312.
[20] J. Haber, M. Witko, J. Catal. 216 (2003) 416.
[21] M. Boudart, G. Djéga-Mariadassou, La cinetique des Reactions en Catalyse Hétérogène, Masson, Paris, 1982, ISBN: 9782225763298;
M. Boudart, G. Djéga-Mariadassou, Kinetics of Heterogeneous Catalytic Reactions, Princeton University Press, Princeton, NJ, 1984, ISBN: 9780691083476.
[22] V.R. Choudhary, B.S. Uphade, S.G. Pataskar, A. Keshavraja, Angew. Chem. Int. Ed. Engl. 35 (1996) 1393.
[23] Y. Liu, S. Wang, T. Sun, D. Gao, C. Zhang, S. Wang, Appl. Catal. B 119–120 (2012) 321.
[24] H. Leion, A. Lyngfelt, T. Mattisson, Chem. Eng. Res. Des. 87 (2009) 1543.
[25] G. Djéga-Mariadassou, M. Boudart, J. Catal. 216 (2003) 89.
[26] M. Maestri, D.G. Vlachos, A. Beretta, G. Groppi, E. Tronconi, J. Catal. 259 (2008) 211.
[27] J.R. Rostrup-Nielsen, J.-H. Bak Hansen, J. Catal. 144 (1993) 38.
[28] S. Chempath, A.T. Bell, J. Catal. 247 (2007) 119.